6th International Conference on Advances in Experimental Structural Engineering
11th International Workshop on Advanced Smart Materials and Smart Structures Technology
August 1-2, 2015, University of Illinois, Urbana-Champaign, United States

# Recent advances on the hybrid simulation of bridges base on partitioned time integration, dynamic identification and model updating

**G. Abbiati[1], E. Cazzador[2], I. Lanese[3], S. Eftekhar Azam[4], O. S. Bursi[2], and A. Pavese[5]**

1. *Department of Civil, Environmental and Geomatic Engineering (D-BAUG), IBK, ETH Zurich Stefano-Franscini-Platz 5, 8093 Zürich, Switzerland e-mail: abbiati@ibk.baug.ethz.ch*
2. *Department of Civil, Environmental and Mechanical Engineering, University of Trento Via Mesiano 77, 38123, Trento, Italy e-mail: oreste.bursi@unitn.it, enrico.cazzador@unitn.it.*
3. *TREES Lab, EUCENTRE European Centre for Training & Research in Earthquake Engineering Via Ferrata 1, 27100 Pavia (PV), Italy e-mail: igor.lanese@eucentre.it*
4. *Department of Mechanical Engineering, University of Thessaly, Volos 38334, Greece, e-mail: eftekhar@uth.gr*
5. *Department of Civil Engineering and Architecture, University of Pavia, Via Ferrata 1, 27100 Pavia (PV), Italy e-mail: a.pavese@unipv.it*

**ABSTRACT**
The influence of the seismic performance of existing bridges on the functionality of communication infrastructures is widely recognized as a crucial issue. Therefore, Hybrid Simulation with Dynamic Substructuring (HS-DS) was selected for assessing the seismic response of a two-pier reinforced concrete (RC) bridge at the Eucentre TREES Laboratory of Pavia (Italy). In order to simulate a consistent degradation between the physical and the numerical pier, the use of the Unscented Kalman Filter as parameter identification tool was explored. A novel parallel partitioned time integrator tailored to first order systems allowed for the straightforward accommodation of the filter.

**KEYWORDS:** *Concrete Bridges, Concave Sliding Bearing, Hybrid Simulation, Partitioned Time Integrators, Unscented Kalman Filter*

## 1. INTRODUCTION

The influence of the seismic performance of existing bridges on the functionality of communication infrastructures is widely recognized as a crucial issue. It is noteworthy that during seismic events the deck response typically lies in the linear range, whilst nonlinear hysteretic responses concentrate on piers and seismic isolators. Hybrid Simulation with Dynamic Substructuring (HS-DS) is particularly well suited for bridge testing [1, 2]. In fact, the Physical Substructure (PS) can be confined to those components where a nonlinear response is expected, whilst the Numerical Substructures (NSs) can be dedicated to linear components.
The present paper summarizes the numerical and the experimental research activities aimed at assessing the seismic response of a reinforced concrete (RC) bridge in both the as built and the isolated configurations. First, the bridge case study is presented. Two hollow cross section concrete columns carried a 135 m long continuous concrete deck. A pair of novel Concave Sliding Bearings (CSBs) were interposed among the deck and each pier and each abutment as a suitable seismic retrofitting scheme. An OpenSees fiber-based Finite Element (FE) model of the bridge was implemented to support the design of the testing campaign. It was used to calibrate a reduced nonlinear state space model implemented for the purpose of HS-DS at the Eucentre TREES Laboratory of Pavia (Italy). A Bouc-Wen spring [3] acted as numerical pier, whilst the Mostaghel bilinear state space model [4] simulated each numerical isolator. In order to facilitate the interoperation between time integration and dynamic identification, a novel partitioned time integration scheme tailored to first order systems is then presented. The use of partitioned time integration tailored to first order systems allowed for the straightforward accommodation of the Unscented Kalman Filter (UKF) as input/output dynamic identification tool. As a result, in some of the tests, the parameters of the Bouc-Wen based S-DoF oscillator representing the numerical pier was identified and updated on line on the basis of the physical pier response. The Eucentre dynamic Bearing Testing System (BTS) was used for the substructuring of one physical full scale CSB and the restoring force of the isolator pair was obtained by doubling the corresponding measurement.

## 2. DESCRIPTION OF THE BRIDGE CASE STUDY

The case study considered is a RC bridge with two hollow section piers supporting the three-spans deck designed with an open section solution. The bridge is composed by three identical spans 45 m length. The case study was tested in both as built and isolated configuration in order to prove the benefit of an isolation system based on CSB. The bridge's deck has a depth of 6.7 m and it is appropriate for a 2-line urban way, as shown in Figures 2.1.

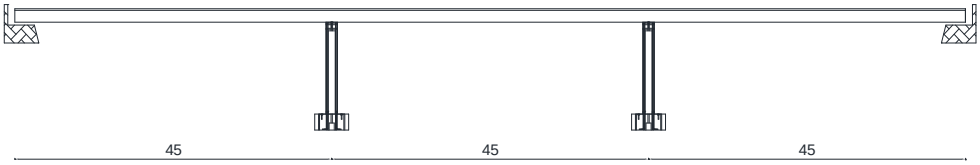


Figure 2.1. Lateral view of the RC Bridge

The geometrical properties of the sections, i.e. pier and deck, are reported in Table 2.1. The complete set of loads in the serviceability condition drop on the pier a load equal to 4000 kN.

Table 2.1 Geometrical properties of cross sections

| | **Deck** | **Pier** |
|---|---|---|
| **Height (H)** | 1.83 m | 1.60 m |
| **Base (B)** | 6.70 m | 3.00 m |
| **Area (A)** | 2.78 $m^2$ | 2.40 $m^2$ |
| **(Iz)** | 7.20 $m^4$ | 0.82 $m^4$ |
| **(Iy)** | 0.85 $m^4$ | 2.40 $m^4$ |

In addition, to investigate the effect of isolation system on this type of bridge, the installation of pairs of CSBs isolation devices positioned between each pier and the deck was considered. In detail, selected CSB devices are characterized by a double-curvature CSB with $3.08\,m$ equivalent radius, $\pm\ 250\,mm$ displacement capacity in all directions and maximum vertical load of $3100\,kN$, designed by Eucentre. An initial stiffness of $150000\,kN/m$ was identified for vertical load of $2000\,kN$, which corresponds to the portion of the self-weight of the bridge deck carried by each device, and the design friction coefficient was $8\,\%$.
The isolation device is a prototype of CSB tested before the PsD tests experimental campaign in the TRESS laboratory of Eucentre, the tests, performed with the uniaxial shaking table, shown an innovative behavior, i.e. asymptotic $\mu_f$ value for higher velocity. Figures 2.2 and 2.3 depicts the a typical hysteretic loop and the friction characterization of the CSB.

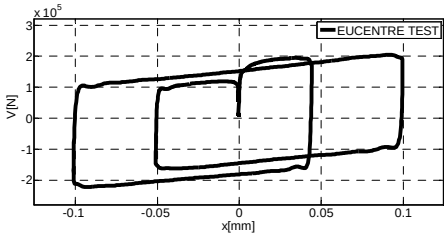


Figure 2.2 Hysteretic loop from Eucentre tests.

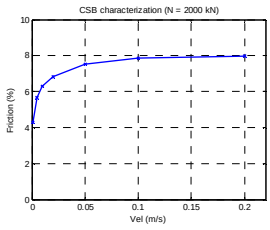


Figure 2.3 CSB friction characterization

With regard to Figure 2.3, a friction coefficient $\mu_f$ equal to $6\%$ corresponded to peak testing velocities. Accordingly, the horizontal restoring force was compensated numerically during HSs.
The input ground motions chosen for the numerical simulations and for the tests are natural accelerograms representative of the seismic zone of Naples. The Italian seismic standards are based on seismic hazard assessment [5]; therefore, on the basis of soil conditions B, Magnitude between 5 and 7 and an epicentral distance of $0-30\,km$ the ground motions were chosen. As a result, an accelerogram with $0.12\,g$ PGA was considered for SLS whilst stronger one with intensity equal to $0.3\,g$ PGA was adopted for the ULS.

## 3. REFINED AND SIMPLIFIED NUMERICAL MODELS OF THE BRIDGE

In order to implement continuous PsD tests, a refined finite element model of the bridge was implemented in the OpenSees environment [6]. Linear beam elements were selected to model the deck, whilst fiber-based non-linear elements were considered for the piers; translational DoFs of both abutments were fixed whilst rotations released. Nonlinear fiber-based beam elements allowed for an accurate discretization of cross sections as well as for positions and dimensions of plain re-bars. On the basis of a previous experimental campaign on the considered 1:2 scale mock-up specimen of Pier #1, in which cyclic quasi-static tests were performed [7], the appropriate materials were implemented in the OpenSees FE model. The contribution of the concrete tensile strength was considered in view of the use of rough steel bars. Therefore, the *Concrete02* material of OpenSees, was employed

to simulate concrete behavior. In detail, we assumed: the maximum concrete strength $fpc = 55\,MPa$ with a corresponding deformation $\varepsilon p = 0.4\%$; the asymptotic concrete strength $fpcu = 44\,MPa$ with a relevant deformation $\varepsilon u = 0.6\%$ and the tensile strength $5.5\,MPa$. Rebars were represented by the *Steel02* material with $fy = 525\,MPa$, along with $E = 200000\,MPa$ and hardening ratio $Ep/E = 0.015$. The frequencies of the first five eigenmodes of the bridge in the as built configuration ranged between 1.56 and 3.12 Hz.
Friction pendulum isolation devices were implemented in OpenSees software by using Friction Pendulum Bearing elements with nominal radius, initial stiffness and vertical load values. *Single Concave Friction Pendulum Bearing* OpenSees elements embed a physical model that replicates the slip mechanism of FPB isolation devices. Numerical simulations of the aforementioned bridge were performed. The seismic response in the as built configuration shown the damage patterns at the ultimate limit state that correspond to the generation of a plastic hinge on the pier's base. The simulations relevant to the isolated case, shown the benefit of the CSB system, in fact the pier response is clearly in the elastic range. The aforementioned OpenSees model was reduced in order to be implemented in the laboratory for the purpose of HS. Figure 3.1 depicts the schematics of both the as built and the isolated state space models.


a) b)

Figure 3.1 Substructuring scheme for the: a) as built; and the b) isolated configuration.

As can be appreciated from Figure 3.1, Pier #1 was substructured in the laboratory together with the related isolator pair. A linear deck was assumed whilst the nonlinear restoring force owing to the lateral displacement of each single pier was simulated by means of the well-known Bouc-Wen model [3]. The formulation of the hysteretic restoring force in differential form reads,

$$\begin{cases} r = \int_0^t \dot{r} d\tau \\ \dot{r} = \left[ A - (\beta \cdot sgn(\dot{x} \cdot r) + \gamma) \,|\, r \,|^n \right] \cdot \dot{x} \end{cases} \tag{3.1}$$

where $\beta, \gamma$ and $n$ are model parameters, whilst $\dot{x}$ and $\dot{r}$ are the velocity and the restoring force rate, respectively. Each substructured pier was considered as a stand-alone Single-Input-Single-Output (SISO) system for the purpose of the identification of the nonlinear parameters $k, \beta$ and $\gamma$; conversely, n was set to 1. Along the same line, the state space model proposed by [4] was selected for reproducing the dynamic substructuring of isolator elements. The expression of the nonlinear restoring force of any nondegenerating bilinear element is given in differential form,

$$\begin{cases} r = \alpha k \cdot x + (1-\alpha) k \cdot u \\ u = \int_0^t \dot{u} d\tau \\ \dot{u} = \left[ \bar{N}(\dot{x}) \bar{M}(u-\delta) + M(\dot{x}) N(u+\delta) \right] \dot{x} \end{cases} \tag{3.2}$$

where $k$ is the total stiffness, $\alpha$ defines the stiffness ratio and $\delta$ represents the system yield displacement. The state variable $u$ refers to the slip displacement; the remaining functions $N, M, \bar{N}$ and $\bar{M}$ are defined as,

$$N(w) = 0.5(1+\mathrm{sgn}(w))\left[1+(1-\mathrm{sgn}(w))\right], M(w) = 1 - N(w), \bar{N}(w) = M(-w), \bar{M}(w) = N(-w) \tag{3.3}$$

Parameters $\alpha, k$ and $\delta$ were tuned based on the OpenSees FE model response.

## 4. THE HYBRID SIMULATION ALGORITHM

Since the same Bouc-Wen model was used for both the simulation of the numerical pier and the dynamic identification of the physical pier, a partitioned time integrator tailored to first order system was selected. Therefore, the following semi-discretized equation of motion was taken as model problem:

$$\mathbf{M}\dot{\mathbf{y}} + \mathbf{G}(\mathbf{y}) = \mathbf{F}(t) \tag{4.1}$$

with,

$$\mathbf{y} = \begin{bmatrix} \mathbf{x} \\ \dot{\mathbf{x}} \end{bmatrix},\ \mathbf{M} = \begin{bmatrix} \mathbf{I} & \mathbf{0} \\ \mathbf{0} & \mathbf{m} \end{bmatrix},\ \mathbf{G}(\mathbf{y}) = \begin{bmatrix} -\mathbf{I} \\ \mathbf{r} \end{bmatrix},\ \mathbf{F}(t) = \begin{bmatrix} \mathbf{0} \\ \mathbf{f}(t) \end{bmatrix} \tag{4.2}$$

In detail, **I** is the identity matrix, whilst **r** is the generic nonlinear restoring force vector and **m** is the mass matrix of the system; **x** and $\dot{\mathbf{x}}$ are displacement and velocity state components, and $\mathbf{f}(t)$ is the external load. In the case of hysteretic restoring force models, the state vector can be easily extended to accommodate additional memory variables. In order to embed favorable user-controlled algorithmic, a modified version of the G-α was considered as basic monolithic integrator for the development of a novel partitioned time integration scheme for hybrid systems. The algorithm relies on velocity-like quantities $\mathbf{v}_n$ that consist of low-pass filtered $\dot{\mathbf{y}}_n$. As a result, the state vector is extended to embed both discretized state variables $\mathbf{y}_n$ and velocity-like quantities $\mathbf{v}_n$. The following equations summarize the time integration procedure of the MG-α method:

$$\mathbf{M}\dot{\mathbf{y}}_{n+1} + \mathbf{G}(\mathbf{y}_{n+1}) = \mathbf{F}_{n+1} \tag{4.3}$$

$$\mathbf{y}_{n+1} = \mathbf{y}_n + \mathbf{v}_n(1-\gamma)\Delta t + \mathbf{v}_{n+1}\gamma\Delta t \tag{4.4}$$

$$(1-\alpha_m)\mathbf{v}_n + \alpha_m\mathbf{v}_{n+1} = (1-\alpha_f)\dot{\mathbf{y}}_n + \alpha_f\dot{\mathbf{y}}_{n+1} + o(\Delta t^2) \tag{4.5}$$

This algorithm is equivalent to its progenitor, i.e. the G-α, in terms of stability, accuracy and spectral properties, but is amenable to hybrid implementations. A novel parallel partitioned time integration scheme based on the MG-α was developed. The coupling scheme of the Modified PH method proposed by [8] was adopted. As well as its progenitor, the proposed algorithm is prone to parallel implementations, where *free problems* advance simultaneously on both subdomains. The task sequence of the Modified PH-method was completely inherited and is depicted in Figure 4.1.

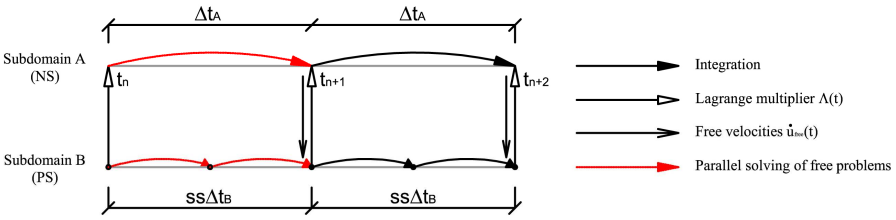


Figure 4.1 Task sequence of the Modified PH-MG-α method.

A coarse time step $\Delta t_A$ was applied to Subdomain A, whilst a fine time $\Delta t_B$ to Subdomain B. Since the link problem is solved at coarse time steps only, interpolated free quantities of Subdomain A are not needed to advance in the solution on Subdomain B. With regard to hybrid simulation, Subdomain B always refers to the PS, where displacement commands are generated at the controller rate. Conversely, Subdomain A refers to the NS, which needs more computational resources and thus larger solving times. Accordingly, discretized coupled equations of motion read,

$$\begin{cases} \mathbf{M}_A \dot{\mathbf{Y}}_{ss}^A + \mathbf{G}_A\left(\mathbf{Y}_{ss}^A\right) + \mathbf{L}_A \boldsymbol{\Lambda}_{ss} = \mathbf{F}_{ss}^A \\ \mathbf{M}_B \dot{\mathbf{Y}}_k^B + \mathbf{G}_B\left(\mathbf{Y}_k^B\right) + \mathbf{L}_B \boldsymbol{\Lambda}_k = \mathbf{F}_k^B \\ \mathbf{B}_A \dot{\mathbf{Y}}_{ss}^A + \mathbf{B}_B \dot{\mathbf{Y}}_{ss}^B = \mathbf{0} \end{cases} \tag{4.6}$$

where $k \in [1,2,\dots,ss]$ and the subcycling parameter $ss$ is defined as $\Delta t_A / \Delta t_B$. Boolean matrices $\mathbf{L}^m$ and $\mathbf{B}^m$localize Lagrange multipliers as interface loads and coupling DoFs, respectively. In order to preserve the stability of underlying monolithic integrators, the compatibility was force on state variable rates, which physically correspond to interface velocities. Accordingly $\mathbf{L}^{m^T} = [\mathbf{0}^T \quad \mathbf{I}^{m^T}]$ and $\mathbf{B}^m = [\mathbf{I}^{m^T} \quad \mathbf{0}]$, where $\mathbf{I}^m$ is a row-wise Boolean matrix that collocates all interface DoFs on the subdomain *m*-th. At each coarse time step $\Delta t_A$, the equation of motion of both subdomains are solved independently.

Owing to the limited length of the paper, please refer to [9] for a detailed description of the solution procedure. In order to preserve the linear stability of underlying monolithic integrators, the Jacobians of $\boldsymbol{G}_A(\cdot)$ and $\boldsymbol{G}_B(\cdot)$ were evaluated beforehand via Automatic-Differentiation (AD). Additional numerical simulations will prove that the resulting partitioned algorithm does not entail interface energy dissipation.

As anticipated, another great advantage of partitioned time integration is that the algorithm provides the interface Lagrange multiplier set at each time step. This means that both input and output loads acting on each subdomain are available. Accordingly, the implementation of any input/output identification tools aimed at characterizing the parameter of a single subdomain is straightforward. In the present implementation, the seismic load acting of the condensed physical pier was moved to the deck subdomain side. In this way, the original dynamics of the bridge was preserved, but Lagrange multipliers were the unique load acting on the physical pier. The presented approach is very suitable for accommodating gray box identification tools, where both the model structure and input and output quantities are available. In fact, Lagrange multipliers $\Lambda_k$ completely characterize the input load acting on the subdomain B. The Unscented Kalman Filter (UKF) was selected in this particular case [10]. In this application, the main mission of the UKF is the online identification of instantaneous system parameters on the basis on the physical pier response.

## 5. DESCRIPTION OF THE TEST SETUP

The scheme of the test setup implemented at the Eucentre TREES Lab, evolution of a previously implemented HS-DS testing system [11], is shown in Figure 5.1.

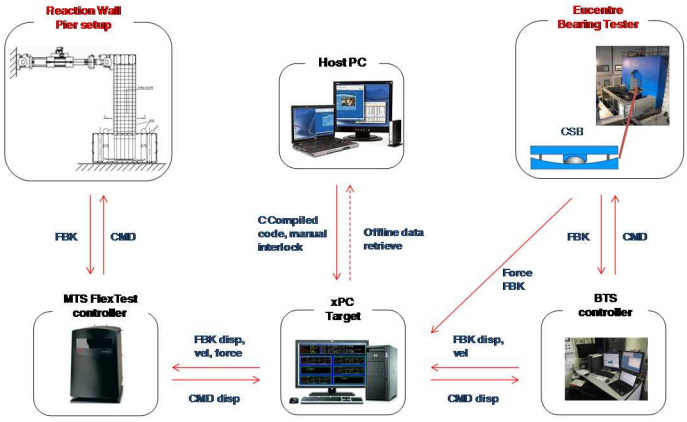


Figure 5.1 Eucentre TREES Lab Hybrid Simulation System Scheme

Both the time integrator and the UKF were implemented in the xPC Target [12] The MTS standard (for the Pier#1 actuator) and customized (for the CSB) controllers are used as secondary inner-loop control to impose the calculated displacement to the specimen and measure corresponding restoring forces. The xPC-Target and MTS controller communicate via analogic signals.

The RC piers of the considered bridge feature structural deficiencies and poor detailing, typical of the old construction practice; in order to accurately catch possible re-bars slip, brittle cracking, failure mechanisms, etc., a 1:2 scale specimen has been realized and used as one of the two physical substructures. Nevertheless, a full-scale prototype model was considered in the simulation. Accordingly, displacement coming from the time

integrator were divided by 2, whilst corresponding restoring forces were multiplied by 4 and then, feedback to the system. In this way, the actual stress/strain expected in the full-scale pier was applied.

a)

b)

Figure 5.2. RC Pier#1 test setup

As shown in Figure 5.2, The RC Pier#1 was fully restrained at the base by 14 Diwidag post-tensioned Ø42 steel bars, while a pin-connection was realized between horizontal actuator and pier cap. The horizontal load has been applied through a 1000 kN dynamic actuator, acting on a post-tensioned system made of two 150 mm thick steel plates positioned on the two sides of the pier cap in the direction of motion (Figure 5.2b). In order to compensate for the flexibility of the pin connection a piecewise linear compensation was implemented for the displacement command. In fact, different stiffness were observed for the tension and the compression of the pins.
The response of the paired CSB devices is represented by one single full-scale CSB, considering a constant vertical load representative of the average conditions of the isolation system. Since the scaling of CSBs produces distortions, because of the modified surface radius, the non-uniform contact pressure, etc., a full-scale specimen was considered. The vertical load due to the self-weight of the bridge deck was kept constant, while horizontal and vertical displacements, univocally related by the surface curvature, are imposed with the Eucentre TREES Lab Bearing Testing System [7]. During open loop tests, the raw shear force of the specimen is measured from horizontal actuators, and then processed afterwards to remove the machine inertia and friction to obtain the device response. This procedure is not compatible with the hybrid simulation requirements, where the restoring force of the specimen has to enter the time integration loop step by step. To this end, a dedicated new restoring force measurement system has been realized as shown in Figure 5.3.

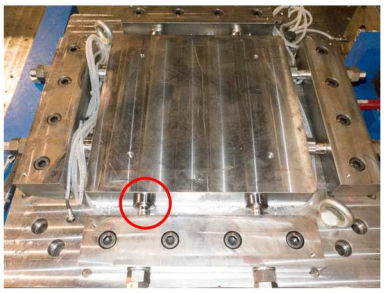

Figure 5.3 CSB direct measurement of the restoring force

The system is made of a steel plate laying on a Teflon layer and surrounded by 8 ring-shaped load cells; because of the negligible friction force at the base, the pre-stressed compression cells directly give the specimen restoring force in two orthogonal plane directions. In order to compensate the velocity effect of the CSB response owing to the extended time scale of the test, the following equation was considered:

$$F_{ALG} = F_H \cdot \frac{f_{hv}}{f_{lv}} - \frac{F_V \cdot D_H}{R_{eq}} \cdot \left(\frac{f_{hv}}{f_{lv}} - 1\right) \tag{5.1}$$

where $F_{ALG}$ is the CSB restoring force computed and sent to the algorithm, $F_H$ is the horizontal restoring force of the CSB, $F_V$ is the vertical load on the CSB, $f_{hv}$ is the friction coefficient at high velocity (about 8%), $f_{lv}$ is the friction coefficient at low (test) velocity (generally about 6%), $D_H$ is the horizontal displacement of the CSB, and $R_{eq}$ is the CSB equivalent radius.

## 6. EXPERIMENTAL RESULTS

The main results of the experimental campaign are summarized hereinafter. In this respect, Table 6.1 reports the list of main tests and related setting.

Table 6.1 Testing program

| Test | Configuration | Time scale $\lambda$ | PGA [g] | PS |
|---|---|---|---|---|
| HE-49 | ISOLATED | 256 | 0.03 | Pier #1 + Iso #2 |
| HE-51 | AS-BUILT | 128 | 0.25 | Pier #1 |
| HE-52 | AS-BUILT | 128 | 0.35 | Pier #1 |
| HE-53 | AS-BUILT | 128 | 0.50 | Pier #1 |
| HE-54 | ISOLATED | 256 | 0.25 | Pier #1 + Iso #2 |
| HE-55 | ISOLATED | 256 | 0.35 | Pier #1 + Iso #2 |
| HE-57 | ISOLATED | 256 | 0.50 | Pier #1 + Iso #2 |
| HE-58 | ISOLATED | 256 | 0.75 | Pier #1 + Iso #2 |
| HE-60 | AS-BUILT | 128 | 0.50 | Pier #1 |
| HE-65 | AS-BUILT | 128 | 0.75 | Pier #1 |
| HE-68 | AS-BUILT | 256 | 0.85 | Pier #1 |

As can be appreciated from Table 6.1, in order to validate the implementation, first, low PGA level tests were conducted in the isolated configuration. Then, three tests have been performed in the as built configuration up to 0.5 g of PGA level. In this way, a slight damage was applied to piers in order to simulate a realistic condition. In order to prove the effectiveness of the proposed retrofitting, isolated tests were conducted afterwards up to 0.75 g of PGA level. Finally, the bridge was simulated in the as built configuration up to 0.85 g of PGA level. Figure 6.1 compares the top displacement vs. force loop of the physical piers in the as built -Test HE-68- and the isolated -Test HE-58- configurations.

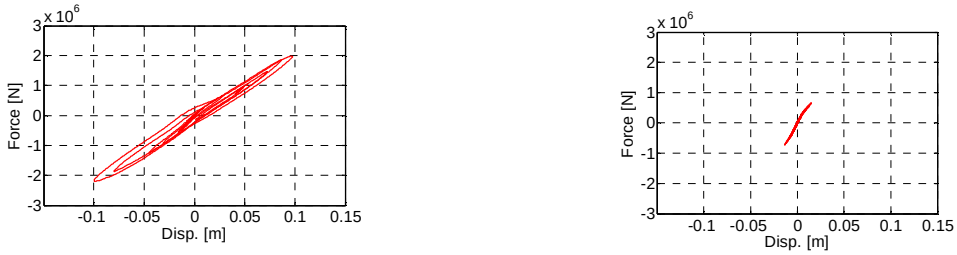


a) b)

Figure 6.1 Hysteretic loops of the physical pier restoring force measured at the top level during tests: a) HE-68 -as built-; and b) HE-58 -isolated-. In both the two cases the PGA level was 0.75 g.

As can be appreciated from Figure 6.1, the proposed seismic isolation scheme strongly reduced the transversal response of piers, which remained in the linear range in the isolated case. The online identification of the parameters of the physical pier and the consistent updating of the numerical pier was confined to the elastic part of the tangent stiffness of the Bouc-Wen model, namely the parameter A. Figure 6.2 depicts the time history of the estimated parameter during test HE-60, which was conducted assuming a PGA level equal to 0.50 g. With regard to the same test, Figure 6.3 compares the hysteretic loops of the restoring forces of both the physical and the numerical piers. As can be appreciated from Figure 6.2, the UKF captured the stiffness degradation of the physical pier that was applied to the numerical pier. Therefore, as can be appreciated from Figure 6.3, a consistent hysteretic response of the numerical pier was simulated.

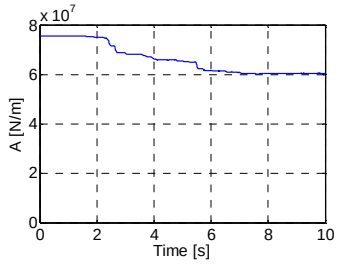


Figure 6.2 Time history of the estimate of the parameter A of the Bouc-Wen spring obtained with the UKF

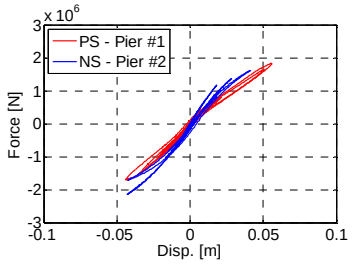


Figure 6.3 Comparison of the hysteretic loops related to the transversal response of both the numerical and the physical piers.

Further numerical simulations showed strong oscillations in the parameter estimate at higher PGA levels, which could hinder the time integration process and indeed, the use of the UKF where a strong nonlinear response is expected is still a matter of research.

## 7. CONCLUSIONS

In order to assess the seismic response of a two-pier reinforced concrete (RC) bridge in both the as built and the isolated configuration, a testing campaign based on Hybrid Simulation with Dynamic Substructuring (HS-DS) was conducted at the Eucentre TREES Laboratory of Pavia (Italy). The Eucentre TREES Lab Bearing Testing System, which has been initially designed to carry out standard qualification tests in force and/or displacement control of isolation devices (CSB, LRB, etc.), was used to substructure a CSB and apply the correct boundary conditions in terms of vertical load and horizontal displacement. In order to simulate a consistent degradation between the physical and the numerical pier in a few tests, the Unscented Kalman Filter was used as dynamic identification tool. A novel parallel partitioned time integrator tailored to first order systems allowed for the straightforward accommodation of the filter.


### ACKNOWLEDGMENT

Eucentre TREES Laboratory of Pavia (Italy), STRIT project funded by the Italian Ministry of Education, Universities and Research (MIUR), RELUIS-DPC 2014-2018 project funded by the Italian Civil Protection Department.


### REFERENCES


1. Pinto A, Pegon P., Magonette G. and Tsionis G. (2004). Pseudo-dynamic testing of bridges using non-linear substructuring. *Earthquake Engineering & Structural Dynamics*, **33(11)**, 1125–1146.
2. Abbiati G., Bursi O. S., Caperan P., Di Sarno L., Molina F. J., Paolacci F., and Pegon P. (2015). Hybrid simulation of a multi-span RC viaduct with plain bars and sliding bearings. *Earthquake Engineering & Structural Dynamics.*
3. Ismail M., Ikhouane F., and Rodellar J. (2009). The Hysteresis Bouc-Wen Model, a Survey. *Archives of Computational Methods in Engineering*, **16(2)**, 161–188.
4. Mostaghel, N. (1999). Analytical Description of Pinching, Degrading Hysteretic Systems. *Journal of Engineering Mechanics*, **125(2)**, 216–224.
5. NTC08 - Decreto Ministeriale 14.01.2008 – Norme tecniche per le costruzioni, 2008 (in Italian).
6. McKenna F, Fenves GL, Scott MH. (2007) OpenSees: open system for earthquake engineering simulation. PEER, University of California: Berkeley.
7. Peloso S. and Pavese A. (2009) Frp Seismic Retrofit For Insufficient Lap-Splice: Large Scale Testing Of Rectangular Hollow Section Bridge Piers. *COMPDYN 2009 ECCOMAS Thematic Conference on Computational Methods in Structural Dynamics and Earthquake Engineering* Rhodes, Greece.
8. Brun M., Batti A, Combescure A, and Gravouil A. (2014). External coupling software based on macro- and micro-time scales for explicit/implicit multi-time-step co-computations in structural dynamics. *Finite Elements in Analysis and Design*, **86**, 101–119.
9. Abbiati G., Bursi O. S., Cazzador E., Pegon P., 2014. An Improved Parallel Partitioned Time Integration Scheme based on the Generalized-α method for Hybrid Simulation. *Proceedings of the 6th World Conference of Structural Control and Monitoring (6WCSCM)*, Barcelona, Spain.
10. Wu, M., & Smyth, A. W. (2007). Application of the unscented Kalman filter for real-time nonlinear structural system identification. Structural Control and Health Monitoring, 14(7), 971-990.
11. Lanese I., (2012) Development and Implementation of an Integrated Architecture for Real-Time Dynamic Hybrid Testing in the Simulation of Seismic Isolated Structures. PhD Dissertation, UME School, IUSS Pavia, Pavia, Italy.
12. MATLAB Release 2012b. The MathWorks, Inc., Natick, Massachusetts, United States.